FERMILAB-PUB-13-329-E

Measurement of associated production of Z bosons with charm quark jets in $p\bar{p}$ collisions at $\sqrt{s} = 1.96$ TeV

V.M. Abazov,[31] B. Abbott,[66] B.S. Acharya,[25] M. Adams,[45] T. Adams,[43] J.P. Agnew,[40] G.D. Alexeev,[31] G. Alkhazov,[35] A. Alton[a],[55] A. Askew,[43] S. Atkins,[53] K. Augsten,[7] C. Avila,[5] F. Badaud,[10] L. Bagby,[44] B. Baldin,[44] D.V. Bandurin,[43] S. Banerjee,[25] E. Barberis,[54] P. Baringer,[52] J.F. Bartlett,[44] U. Bassler,[15] V. Bazterra,[45] A. Bean,[52] M. Begalli,[2] L. Bellantoni,[44] S.B. Beri,[23] G. Bernardi,[14] R. Bernhard,[19] I. Bertram,[38] M. Besançon,[15] R. Beuselinck,[39] P.C. Bhat,[44] S. Bhatia,[57] V. Bhatnagar,[23] G. Blazey,[46] S. Blessing,[43] K. Bloom,[58] A. Boehnlein,[44] D. Boline,[63] E.E. Boos,[33] G. Borissov,[38] A. Brandt,[69] O. Brandt,[20] R. Brock,[56] A. Bross,[44] D. Brown,[14] X.B. Bu,[44] M. Buehler,[44] V. Buescher,[21] V. Bunichev,[33] S. Burdin[b],[38] C.P. Buszello,[37] E. Camacho-Pérez,[28] B.C.K. Casey,[44] H. Castilla-Valdez,[28] S. Caughron,[56] S. Chakrabarti,[63] K.M. Chan,[50] A. Chandra,[71] E. Chapon,[15] G. Chen,[52] S.W. Cho,[27] S. Choi,[27] B. Choudhary,[24] S. Cihangir,[44] D. Claes,[58] J. Clutter,[52] M. Cooke,[44] W.E. Cooper,[44] M. Corcoran,[71] F. Couderc,[15] M.-C. Cousinou,[12] D. Cutts,[68] A. Das,[41] G. Davies,[39] S.J. de Jong,[29,30] E. De La Cruz-Burelo,[28] F. Déliot,[15] R. Demina,[62] D. Denisov,[44] S.P. Denisov,[34] S. Desai,[44] C. Deterre[d],[20] K. DeVaughan,[58] H.T. Diehl,[44] M. Diesburg,[44] P.F. Ding,[40] A. Dominguez,[58] A. Dubey,[24] L.V. Dudko,[33] A. Duperrin,[12] S. Dutt,[23] M. Eads,[46] D. Edmunds,[56] J. Ellison,[42] V.D. Elvira,[44] Y. Enari,[14] H. Evans,[48] V.N. Evdokimov,[34] L. Feng,[46] T. Ferbel,[62] F. Fiedler,[21] F. Filthaut,[29,30] W. Fisher,[56] H.E. Fisk,[44] M. Fortner,[46] H. Fox,[38] S. Fuess,[44] A. Garcia-Bellido,[62] J.A. García-González,[28] V. Gavrilov,[32] W. Geng,[12,56] C.E. Gerber,[45] Y. Gershtein,[59] G. Ginther,[44,62] G. Golovanov,[31] P.D. Grannis,[63] S. Greder,[16] H. Greenlee,[44] G. Grenier,[17] Ph. Gris,[10] J.-F. Grivaz,[13] A. Grohsjean[c],[15] S. Grünendahl,[44] M.W. Grünewald,[26] T. Guillemin,[13] G. Gutierrez,[44] P. Gutierrez,[66] J. Haley,[54] L. Han,[4] K. Harder,[40] A. Harel,[62] J.M. Hauptman,[51] J. Hays,[39] T. Head,[40] T. Hebbeker,[18] D. Hedin,[46] H. Hegab,[67] A.P. Heinson,[42] U. Heintz,[68] C. Hensel,[20] I. Heredia-De La Cruz[d],[28] K. Herner,[44] G. Hesketh[f],[40] M.D. Hildreth,[50] R. Hirosky,[72] T. Hoang,[43] J.D. Hobbs,[63] B. Hoeneisen,[9] J. Hogan,[71] M. Hohlfeld,[21] J.L. Holzbauer,[57] I. Howley,[69] Z. Hubacek,[7,15] V. Hynek,[7] I. Iashvili,[61] Y. Ilchenko,[70] R. Illingworth,[44] A.S. Ito,[44] S. Jabeen,[68] M. Jaffré,[13] A. Jayasinghe,[66] M.S. Jeong,[27] R. Jesik,[39] P. Jiang,[4] K. Johns,[41] E. Johnson,[56] M. Johnson,[44] A. Jonckheere,[44] P. Jonsson,[39] J. Joshi,[42] A.W. Jung,[44] A. Juste,[36] E. Kajfasz,[12] D. Karmanov,[33] I. Katsanos,[58] R. Kehoe,[70] S. Kermiche,[12] N. Khalatyan,[44] A. Khanov,[67] A. Kharchilava,[61] Y.N. Kharzheev,[31] I. Kiselevich,[32] J.M. Kohli,[23] A.V. Kozelov,[34] J. Kraus,[57] A. Kumar,[61] A. Kupco,[8] T. Kurča,[17] V.A. Kuzmin,[33] S. Lammers,[48] P. Lebrun,[17] H.S. Lee,[27] S.W. Lee,[51] W.M. Lee,[43] X. Lei,[41] J. Lellouch,[14] D. Li,[14] H. Li,[72] L. Li,[42] Q.Z. Li,[44] J.K. Lim,[27] D. Lincoln,[44] J. Linnemann,[56] V.V. Lipaev,[34] R. Lipton,[44] H. Liu,[70] Y. Liu,[4] A. Lobodenko,[35] M. Lokajicek,[8] R. Lopes de Sa,[63] R. Luna-Garcia[g],[28] A.L. Lyon,[44] A.K.A. Maciel,[1] R. Madar,[19] R. Magaña-Villalba,[28] S. Malik,[58] V.L. Malyshev,[31] J. Mansour,[20] J. Martínez-Ortega,[28] R. McCarthy,[63] C.L. McGivern,[40] M.M. Meijer,[29,30] A. Melnitchouk,[44] D. Menezes,[46] P.G. Mercadante,[3] M. Merkin,[33] A. Meyer,[18] J. Meyer[i],[20] F. Miconi,[16] N.K. Mondal,[25] M. Mulhearn,[72] E. Nagy,[12] M. Narain,[68] R. Nayyar,[41] H.A. Neal,[55] J.P. Negret,[5] P. Neustroev,[35] H.T. Nguyen,[72] T. Nunnemann,[22] J. Orduna,[71] N. Osman,[12] J. Osta,[50] A. Pal,[69] N. Parashar,[49] V. Parihar,[68] S.K. Park,[27] R. Partridge[e],[68] N. Parua,[48] A. Patwa[j],[64] B. Penning,[44] M. Perfilov,[33] Y. Peters,[20] K. Petridis,[40] G. Petrillo,[62] P. Pétroff,[13] M.-A. Pleier,[64] V.M. Podstavkov,[44] A.V. Popov,[34] M. Prewitt,[71] D. Price,[48] N. Prokopenko,[34] J. Qian,[55] A. Quadt,[20] B. Quinn,[57] P.N. Ratoff,[38] I. Razumov,[34] I. Ripp-Baudot,[16] F. Rizatdinova,[67] M. Rominsky,[44] A. Ross,[38] C. Royon,[15] P. Rubinov,[44] R. Ruchti,[50] G. Sajot,[11] A. Sánchez-Hernández,[28] M.P. Sanders,[22] A.S. Santos[h],[1] G. Savage,[44] L. Sawyer,[53] T. Scanlon,[39] R.D. Schamberger,[63] Y. Scheglov,[35] H. Schellman,[47] C. Schwanenberger,[40] R. Schwienhorst,[56] J. Sekaric,[52] H. Severini,[66] E. Shabalina,[20] V. Shary,[15] S. Shaw,[56] A.A. Shchukin,[34] V. Simak,[7] P. Skubic,[66] P. Slattery,[62] D. Smirnov,[50] G.R. Snow,[58] J. Snow,[65] S. Snyder,[64] S. Söldner-Rembold,[40] L. Sonnenschein,[18] K. Soustruznik,[6] J. Stark,[11] D.A. Stoyanova,[34] M. Strauss,[66] L. Suter,[40] P. Svoisky,[66] M. Titov,[15] V.V. Tokmenin,[31] Y.-T. Tsai,[62] D. Tsybychev,[63] B. Tuchming,[15] C. Tully,[60] L. Uvarov,[35] S. Uvarov,[35] S. Uzunyan,[46] R. Van Kooten,[48] W.M. van Leeuwen,[29] N. Varelas,[45] E.W. Varnes,[41] I.A. Vasilyev,[34] A.Y. Verkheev,[31] L.S. Vertogradov,[31] M. Verzocchi,[44] M. Vesterinen,[40] D. Vilanova,[15] P. Vokac,[7] H.D. Wahl,[43] M.H.L.S. Wang,[44] J. Warchol,[50] G. Watts,[73] M. Wayne,[50] J. Weichert,[21] L. Welty-Rieger,[47] M.R.J. Williams,[48] G.W. Wilson,[52] M. Wobisch,[53] D.R. Wood,[54] T.R. Wyatt,[40] Y. Xie,[44] R. Yamada,[44]

Operated by Fermi Research Alliance, LLC under Contract No. De-AC02-07CH11359 with the United States Department of Energy.

S. Yang,[4] T. Yasuda,[44] Y.A. Yatsunenko,[31] W. Ye,[63] Z. Ye,[44] H. Yin,[44] K. Yip,[64] S.W. Youn,[44] J.M. Yu,[55] J. Zennamo,[61] T.G. Zhao,[40] B. Zhou,[55] J. Zhu,[55] M. Zielinski,[62] D. Zieminska,[48] and L. Zivkovic[14]

(The D0 Collaboration*)

[1]*LAFEX, Centro Brasileiro de Pesquisas Físicas, Rio de Janeiro, Brazil*
[2]*Universidade do Estado do Rio de Janeiro, Rio de Janeiro, Brazil*
[3]*Universidade Federal do ABC, Santo André, Brazil*
[4]*University of Science and Technology of China, Hefei, People's Republic of China*
[5]*Universidad de los Andes, Bogotá, Colombia*
[6]*Charles University, Faculty of Mathematics and Physics, Center for Particle Physics, Prague, Czech Republic*
[7]*Czech Technical University in Prague, Prague, Czech Republic*
[8]*Institute of Physics, Academy of Sciences of the Czech Republic, Prague, Czech Republic*
[9]*Universidad San Francisco de Quito, Quito, Ecuador*
[10]*LPC, Université Blaise Pascal, CNRS/IN2P3, Clermont, France*
[11]*LPSC, Université Joseph Fourier Grenoble 1, CNRS/IN2P3, Institut National Polytechnique de Grenoble, Grenoble, France*
[12]*CPPM, Aix-Marseille Université, CNRS/IN2P3, Marseille, France*
[13]*LAL, Université Paris-Sud, CNRS/IN2P3, Orsay, France*
[14]*LPNHE, Universités Paris VI and VII, CNRS/IN2P3, Paris, France*
[15]*CEA, Irfu, SPP, Saclay, France*
[16]*IPHC, Université de Strasbourg, CNRS/IN2P3, Strasbourg, France*
[17]*IPNL, Université Lyon 1, CNRS/IN2P3, Villeurbanne, France and Université de Lyon, Lyon, France*
[18]*III. Physikalisches Institut A, RWTH Aachen University, Aachen, Germany*
[19]*Physikalisches Institut, Universität Freiburg, Freiburg, Germany*
[20]*II. Physikalisches Institut, Georg-August-Universität Göttingen, Göttingen, Germany*
[21]*Institut für Physik, Universität Mainz, Mainz, Germany*
[22]*Ludwig-Maximilians-Universität München, München, Germany*
[23]*Panjab University, Chandigarh, India*
[24]*Delhi University, Delhi, India*
[25]*Tata Institute of Fundamental Research, Mumbai, India*
[26]*University College Dublin, Dublin, Ireland*
[27]*Korea Detector Laboratory, Korea University, Seoul, Korea*
[28]*CINVESTAV, Mexico City, Mexico*
[29]*Nikhef, Science Park, Amsterdam, the Netherlands*
[30]*Radboud University Nijmegen, Nijmegen, the Netherlands*
[31]*Joint Institute for Nuclear Research, Dubna, Russia*
[32]*Institute for Theoretical and Experimental Physics, Moscow, Russia*
[33]*Moscow State University, Moscow, Russia*
[34]*Institute for High Energy Physics, Protvino, Russia*
[35]*Petersburg Nuclear Physics Institute, St. Petersburg, Russia*
[36]*Institució Catalana de Recerca i Estudis Avançats (ICREA) and Institut de Física d'Altes Energies (IFAE), Barcelona, Spain*
[37]*Uppsala University, Uppsala, Sweden*
[38]*Lancaster University, Lancaster LA1 4YB, United Kingdom*
[39]*Imperial College London, London SW7 2AZ, United Kingdom*
[40]*The University of Manchester, Manchester M13 9PL, United Kingdom*
[41]*University of Arizona, Tucson, Arizona 85721, USA*
[42]*University of California Riverside, Riverside, California 92521, USA*
[43]*Florida State University, Tallahassee, Florida 32306, USA*
[44]*Fermi National Accelerator Laboratory, Batavia, Illinois 60510, USA*
[45]*University of Illinois at Chicago, Chicago, Illinois 60607, USA*
[46]*Northern Illinois University, DeKalb, Illinois 60115, USA*
[47]*Northwestern University, Evanston, Illinois 60208, USA*
[48]*Indiana University, Bloomington, Indiana 47405, USA*
[49]*Purdue University Calumet, Hammond, Indiana 46323, USA*
[50]*University of Notre Dame, Notre Dame, Indiana 46556, USA*
[51]*Iowa State University, Ames, Iowa 50011, USA*
[52]*University of Kansas, Lawrence, Kansas 66045, USA*
[53]*Louisiana Tech University, Ruston, Louisiana 71272, USA*
[54]*Northeastern University, Boston, Massachusetts 02115, USA*
[55]*University of Michigan, Ann Arbor, Michigan 48109, USA*
[56]*Michigan State University, East Lansing, Michigan 48824, USA*
[57]*University of Mississippi, University, Mississippi 38677, USA*
[58]*University of Nebraska, Lincoln, Nebraska 68588, USA*

[59]Rutgers University, Piscataway, New Jersey 08855, USA
[60]Princeton University, Princeton, New Jersey 08544, USA
[61]State University of New York, Buffalo, New York 14260, USA
[62]University of Rochester, Rochester, New York 14627, USA
[63]State University of New York, Stony Brook, New York 11794, USA
[64]Brookhaven National Laboratory, Upton, New York 11973, USA
[65]Langston University, Langston, Oklahoma 73050, USA
[66]University of Oklahoma, Norman, Oklahoma 73019, USA
[67]Oklahoma State University, Stillwater, Oklahoma 74078, USA
[68]Brown University, Providence, Rhode Island 02912, USA
[69]University of Texas, Arlington, Texas 76019, USA
[70]Southern Methodist University, Dallas, Texas 75275, USA
[71]Rice University, Houston, Texas 77005, USA
[72]University of Virginia, Charlottesville, Virginia 22904, USA
[73]University of Washington, Seattle, Washington 98195, USA

(Dated: August 20, 2013)

We present the first measurements of the ratios of cross sections, $\sigma(p\bar{p} \to Z{+}c\,\text{jet})/\sigma(p\bar{p} \to Z{+}\text{jet})$ and $\sigma(p\bar{p} \to Z + c\text{ jet})/\sigma(p\bar{p} \to Z + b\text{ jet})$ for the associated production of a Z boson with at least one charm or bottom quark jet. Jets have transverse momentum $p_T^{\text{jet}} > 20$ GeV and pseudorapidity $|\eta^{\text{jet}}| < 2.5$. These cross section ratios are measured differentially as a function of jet and Z boson transverse momenta, based on 9.7 fb^{-1} of $p\overline{p}$ collisions collected with the D0 detector at the Fermilab Tevatron Collider at $\sqrt{s} = 1.96$ TeV. The measurements show significant deviations from perturbative QCD calculations and predictions from various event generators.

PACS numbers: 12.38.Qk, 13.85.Qk, 14.65.Dw, 14.70.Hp

Studies of Z boson production in association with heavy flavor (HF) jets originating from b or c quarks provide important tests of perturbative quantum chromodynamics (pQCD) calculations [1]. A good theoretical description of these processes is essential since they form a major background for a variety of physics processes, including standard model Higgs boson production in association with a Z boson, $ZH(H \to b\bar{b})$ [2]. Furthermore, the relative contributions of the different flavors to the background is important since $Z + c$ jet events can be misidentified as $Z + b$ jet events, or vice versa, and therefore introduce additional uncertainties into measurements.

The ratio of $Z + b$ jet to inclusive $Z +$ jet production cross sections for events with one or more jets has previously been measured by the CDF [3, 4] and D0 [5, 6] Collaborations. This Letter reports the first measurement of associated charm jet production with a Z boson. In particular, we present the measurement of the ratio of cross sections for $Z + c$ jet to $Z +$ jet production as well as $Z + c$ jet to $Z + b$ jet production in events with at least one jet. The measurement of the ratio of cross sections benefits from the cancellation of several systematic uncertainties and therefore allows for a more precise comparison of data with the theoretical predictions. These ratio measurements are also presented differentially as a function of the transverse momenta of the jet (p_T^{jet}) and Z boson (p_T^Z).

The current analysis is based on the complete Run II data sample collected using the D0 detector [7] at Fermilab's Tevatron $p\overline{p}$ Collider with a center-of-mass energy of 1.96 TeV, and corresponds to an integrated luminosity of 9.7 fb^{-1} following the application of relevant data quality requirements. We use the same triggering, selections, object reconstruction, and event modeling as described in the recent D0 measurement of $Z + b$ jet production [6], but with a dedicated strategy for the extraction of the c-jet fraction. Events must contain a $Z \to \ell\ell$ candidate with a dilepton invariant mass in the range $70 < M_{\ell\ell} < 110$ GeV ($\ell = e, \mu$).

Dielectron (ee) events are required to have two electrons, with no requirement on the sign of their electric charge, with transverse momentum $p_T >$ 15 GeV identified through electromagnetic (EM) showers in the calorimeter. One electron must be identified in the central calorimeter (CC), within a pseudorapidity [8] region $|\eta| < 1.1$, while the second electron can be reconstructed either in the CC or the endcap calorimeters, $1.5 < |\eta| < 2.5$. Dimuon ($\mu\mu$) events are required to have two oppositely charged muons, with $p_T >$ 15 GeV and $|\eta| < 2$, detected in the muon spectrometer and matched to central tracker tracks. In addition, at least one hadronic jet must be reconstructed in the event us-

*with visitors from [a]Augustana College, Sioux Falls, SD, USA, [b]The University of Liverpool, Liverpool, UK, [c]DESY, Hamburg, Germany, [d]Universidad Michoacana de San Nicolas de Hidalgo, Morelia, Mexico [e]SLAC, Menlo Park, CA, USA, [f]University College London, London, UK, [g]Centro de Investigacion en Computacion - IPN, Mexico City, Mexico, [h]Universidade Estadual Paulista, São Paulo, Brazil, [i]Karlsruher Institut für Technologie (KIT) - Steinbuch Centre for Computing (SCC) and [j]Office of Science, U.S. Department of Energy, Washington, D.C. 20585, USA.

ing an iterative midpoint cone algorithm [9] with a cone size of $\Delta R = \sqrt{(\Delta\varphi)^2 + (\Delta y)^2} = 0.5$ where φ is the azimuthal angle and y is the rapidity. This jet must satisfy $p_T^{\rm jet} > 20$ GeV and $|\eta^{\rm jet}| < 2.5$.

Several processes can mimic the signature of $Z+$jet events. These include top quark pair ($t\bar{t}$), diboson (WW, WZ, and ZZ), and multijet production. To suppress the contributions from $t\bar{t}$ production, events with significant imbalance in the measured transverse energy, $\not\!\!E_T$, due to undetected neutrinos from the W boson decay ($t \to Wb \to \ell\nu_\ell b$), are rejected if $\not\!\!E_T > 60$ GeV. These selection criteria retain an inclusive sample of 176,498 $Z+$jet event candidates in the ee and $\mu\mu$ channels.

To estimate acceptances, efficiencies, and backgrounds, the $Z+$jet events (including HF jets) and $t\bar{t}$ events are modeled by ALPGEN [10], which generates sub-processes using higher-order QCD tree-level matrix elements (ME), interfaced with the PYTHIA Monte Carlo (MC) event generator [11] for parton showering and hadronization and EVTGEN [12] for modeling the decay of particles containing b and c quarks. Inclusive diboson production is simulated with PYTHIA. The CTEQ6L1 [13] parton distribution functions (PDFs) are used in these simulations and the cross sections are scaled to the corresponding higher-order theoretical calculations. For the diboson and $Z+$jet processes, including $Z+b\bar{b}$ and $Z+c\bar{c}$ production, next-to-leading order (NLO) cross section predictions are taken from MCFM [14]. The $t\bar{t}$ cross section is determined from approximate next-to-NLO calculations [15]. To improve the modeling of the p_T distribution of the Z boson, simulated $Z+$jet events are also reweighted to be consistent with the measured p_T spectrum of Z bosons observed in data [16]. The multijet background, where jets are misidentified as leptons, is determined using a data-driven method, as described in the recent D0 publication [6]. The fractions of non-$Z+$jet events in the ee and $\mu\mu$ samples are about 9.6% and 1.3%, respectively. These fractions are dominated by multijet production where a jet is either mis-reconstructed as a lepton in the electron channel, or a lepton from decays of hadrons in a jet that passes the isolation requirement, in the muon channel.

This analysis employs a two-step procedure to determine the HF content of jets in the selected $Z+$jet events. We employ a HF tagging algorithm [17] to enrich the sample in b and c jets. The b, c, and light jet composition of the data is then extracted via a template-based fit.

Jets considered for HF tagging are subject to a preselection requirement, known as taggability [17] to decouple the intrinsic performance of the HF jet tagging algorithm from effects related to track reconstruction efficiency. For this purpose, the jet is required to have at least two associated tracks with $p_T > 0.5$ GeV and the highest-p_T track must have $p_T > 1$ GeV. The efficiency of the taggability requirement is 90% for both c and b jets.

The HF tagging algorithm is based on a multivariate analysis (MVA) technique [18] that provides an improved performance over the neural network HF tagging discriminant, described in Ref. [17], used in earlier D0 analyses. This new algorithm, known as MVA$_{bl}$, also utilizes the relatively long lifetime of HF hadrons with respect to their lighter counterparts. Events with at least one jet passing the HF tagging selection are considered in the analysis.

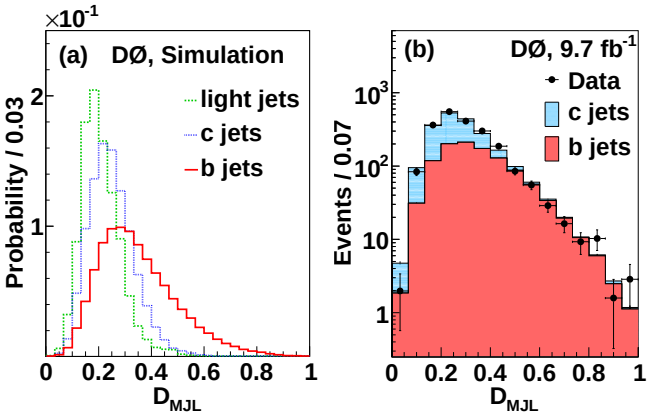

FIG. 1: (color online) (a) The probability densities of the $D_{\rm MJL}$ discriminant for b, c, and light jets passing the final selection requirements. These templates are obtained from MC. (b) The $D_{\rm MJL}$ discriminant distribution of events in the combined sample after background subtraction. The distributions of the b and c jets are weighted by the fractions found from the fit. Uncertainties are statistical only.

To extract the fraction of different flavor jets in the data sample, a second discriminant, $D_{\rm MJL}$, is employed, which offers improved flavor separation for jets passing our MVA$_{bl}$ requirement [6]. It is a combination of two discriminating variables, the secondary vertex mass ($M_{\rm SV}$) and the jet lifetime impact parameter (JLIP) [17]: $D_{\rm MJL} = 0.5 \times (M_{\rm SV}/5\ {\rm GeV} - \ln({\rm JLIP})/20)$. The coefficients in this expression are chosen to optimize the separation of the HF and light quark components. Fig. 1(a) shows the $D_{\rm MJL}$ distributions (templates) obtained from simulations of all three considered jet flavors that pass an MVA$_{bl} > 0.5$ requirement.

To measure the relative fraction of c jets in the HF enriched sample, the following two approaches were considered. The first is based on the methods used in Ref. [6] where the composition of b, c, and light jets is extracted by fitting MC templates to the data. This approach yields a large uncertainty on the c-jet fraction since the $D_{\rm MJL}$ distributions of c and light jets are similar. The second approach is to suppress events with light jets by employing a more stringent MVA$_{bl}$ requirement. The remaining small $Z+$light jet contribution, as estimated with data-corrected simulations, is then subtracted from the data. This allows for the data to be fit with only

b and c jet templates. Both methods yield consistent results, but the second method benefits from a reduced overall uncertainty since only the normalization of b and c jet templates are allowed to vary when fitting the data. Events are retained for further analysis if they contain at least one jet with an MVA$_{bl}$ output greater than 0.5. After these requirements, 2,665 Z + jet events are selected where only the highest-p_T HF tagged jet is examined. The efficiencies of the MVA$_{bl}$ selection for b and c jets, and the light jet misidentification rate are 40%, 9.0%, and 0.24%, respectively. The background is dominated by Z+light jet events that comprise 12% of the total sample. Before the two parameter fit, all background components are subtracted from the data, yielding a sample of 2,125 events.

We measure the fraction of events that contain at least one b or c jet in the ee and $\mu\mu$ samples separately, yielding c jet flavor fractions of $0.509 \pm 0.041\,(\text{stat.})$ and $0.470 \pm 0.039\,(\text{stat.})$, respectively. Since these are consistent and the kinematics of the corresponding events are similar, we combine the two samples to increase the statistical power of the fit. The combined $D_{\rm MJL}$ distribution of the HF-enriched background subtracted data and the fitted templates for the b and c jets are shown in Fig. 1(b). The corresponding fractions of c and b jets in the data are found to be $0.486 \pm 0.027\,(\text{stat.})$ and $0.514 \pm 0.027\,(\text{stat.})$, respectively. These fractions are combined with the relevant detector acceptances and efficiencies to determine the ratios of cross sections using

$$\begin{aligned} R_{c/\rm jet} &\equiv \frac{\sigma(Z{+}c\text{ jet})}{\sigma(Z{+}\text{jet})} = \frac{N_{\rm HF} f_c}{N_{\rm incl}\,\epsilon^c_{tag}} \times \frac{\mathcal{A}_{\rm incl}}{\mathcal{A}_c} \\ R_{c/b} &\equiv \frac{\sigma(Z{+}c\text{ jet})}{\sigma(Z{+}b\text{ jet})} = \frac{f_c\ \epsilon^c_{tag}}{f_b\ \epsilon^b_{tag}} \times \frac{\mathcal{A}_b}{\mathcal{A}_c} \end{aligned} \quad (1)$$

where $N_{\rm incl}$ is the total number of Z + jet events before the tagging requirements, $N_{\rm HF}$ is the number of Z + jet events used in the $D_{\rm MJL}$ fit, $f_{b(c)}$ is the extracted $b(c)$ jet fraction, and $\epsilon^{b(c)}_{tag}$ is the selection efficiency for $b(c)$ jets, which combines the efficiencies for taggability and MVA$_{bl}$ discriminant selection. $N_{\rm incl}$ and $N_{\rm HF}$ correspond to the number of events that remain after the contributions from various background processes have been subtracted. We subtract contributions from $t\bar{t}$, diboson, and multijet production to obtain $N_{\rm incl}$, while we also subtract the Z + light jet events when calculating $N_{\rm HF}$.

The detector acceptances for the inclusive jet, $\mathcal{A}_{\rm incl}$, and $b(c)$ jets, $\mathcal{A}_{b(c)}$, are determined from MC simulation in the kinematic region that satisfies the p_T and η requirements for leptons and jets. In these ratios, the effect of migration of events near the kinematic thresholds, or between neighboring kinematic bins, due to detector resolution is found to be negligible.

Using Eqs. (1), the ratio of the cross sections $Z + c$ jet to inclusive Z + jet in the combined $\mu\mu$ and ee channel, $R_{c/\rm jet}$, is $0.0829 \pm 0.0052\,(\text{stat.})$ and the ratio of cross sections $Z + c$ jet to $Z + b$ jet, $R_{c/b}$, is found to be $4.00 \pm 0.21\,(\text{stat.})$. These ratios have also been measured differentially as a function of $p_T^{\rm jet}$ and p_T^Z. For $R_{c/\rm jet}$, the highest-p_T tagged jet from the HF enriched sample is used in the numerator, while the denominator uses the highest-p_T jet from the Z + jet sample. The selected bin sizes along with the corresponding statistics of data events are listed in Table I. In each case, all the quantities that enter into Eqs. (1) are determined in each bin separately.

TABLE I: Summary of bins, data statistics and the measured ratios along with the statistical and systematic relative uncertainties in percent. Bin centers, shown in parenthesis, are chosen using the prescription in Ref. [19].

$p_T^{\rm jet}$ [GeV]	N	$R_{c/\rm jet}$	Stat. [%]	Syst. [%]	$R_{c/b}$	Stat. [%]	Syst. [%]
$20-30\,(24.6)$	741	0.068	12	16	3.64	8.5	21
$30-40\,(34.3)$	525	0.084	11	12	3.97	8.3	14
$40-60\,(47.3)$	474	0.099	11	9.1	3.98	10	13
$60-200\,(78.0)$	380	0.085	13	11	4.30	13	14
p_T^Z [GeV]							
$0-20\,(10.2)$	285	0.041	29	22	1.15	26	32
$20-40\,(29.5)$	763	0.073	8.2	12	6.10	8.2	20
$40-60\,(49.0)$	588	0.104	10	11	5.06	10	15
$60-200\,(92.7)$	487	0.108	13	8.3	3.41	13	13

Several systematic uncertainties cancel when the ratios are measured. These include uncertainties on the luminosity measurement, as well as trigger, lepton, and the jet reconstruction efficiencies. The remaining uncertainties are estimated separately for the integrated and differential results. For the two ratios the systematic uncertainties are estimated separately.

For the integrated $R_{c/\rm jet}$ measurement, the largest systematic uncertainty of 8.1% comes from the estimation of the Z + light jet background. This is quantified by comparing the value extracted from the data, using a three template (light, c, and b jet) fit, for various MVA$_{bl}$ selections. The next largest systematic uncertainty comes from the shape of the $D_{\rm MJL}$ templates used in the fit. A variety of different aspects can affect the shape of the templates: two HF jets being reconstructed as a single jet; models of b and c quark fragmentation; the background from the non-Z + jet events; the difference in the shape of the light jet MC template and a template derived from a light jet enriched dijet data sample; and the uncertainty of shape of the templates due to MC statistics. These are all evaluated by varying the central values by the corresponding uncertainties, one at a time, and repeating the entire analysis chain, resulting in a 5.5% uncertainty. An additional uncertainty of 3.4% comes from jet energy calibration; it comprises the uncertainties on the jet energy resolution and the jet energy scale. An uncertainty is also associated with the c jet tagging efficiency (1.9%) [17]. Finally, a

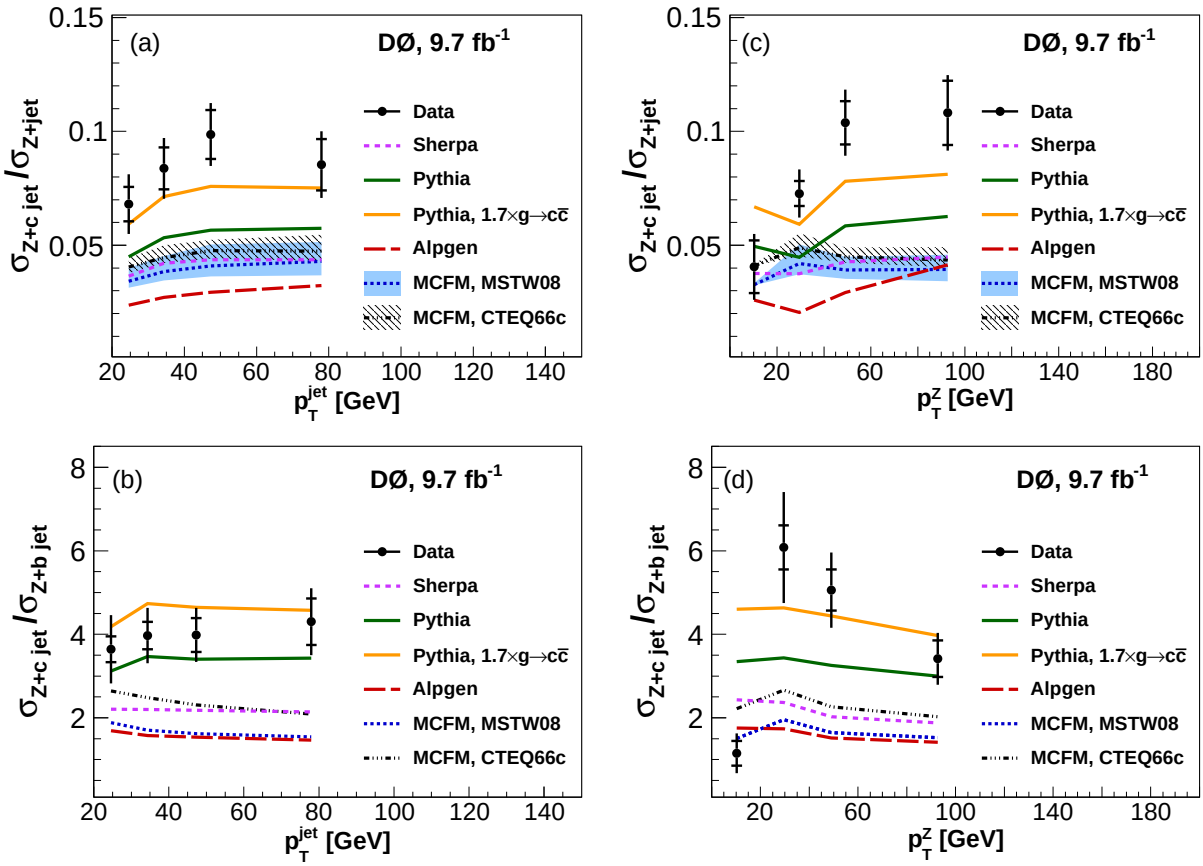

FIG. 2: (color online) Ratios of the differential cross sections $R_{c/\mathrm{jet}}$ and $R_{c/b}$ as a function of (a,b) p_T^{jet} and (c,d) p_T^Z, respectively. The uncertainties on the data include statistical (inner error bar) and full uncertainties (entire error bar). The predictions from ALPGEN, SHERPA, PYTHIA, PYTHIA with an enhanced $g \to c\bar{c}$ component, and MCFM NLO with the MSTW2008 and the CTEQ6.6c PDFs are also shown. The bands represent variations of the scales up and down by a factor of two.

small contribution ($< 0.1\%$) is coming from the dependence of the acceptance on modeling of the signal events. When summed in quadrature the total systematic uncertainty for the integrated $R_{c/\mathrm{jet}}$ ratio is 10.6%. The corresponding total systematic uncertainty is 14.4% for $R_{c/b}$. Table I lists the total statistical and systematic uncertainties (added in quadrature) for the differential results. Finally, for the integrated ratios we obtain values of $R_{c/\mathrm{jet}} = 0.0829 \pm 0.0052\,(\mathrm{stat.}) \pm 0.0089\,(\mathrm{syst.})$ and $R_{c/b} = 4.00 \pm 0.21\,(\mathrm{stat.}) \pm 0.58\,(\mathrm{syst.})$.

The measurements are compared to predictions from an MCFM NLO pQCD calculation and three MC event generators, SHERPA [20], PYTHIA, and ALPGEN. The NLO predictions are based on MCFM [1], version 6.3, with the MSTW2008 PDFs [21] and the renormalization and factorization scales set at $\mu_R^2 = \mu_F^2 = M_Z^2 + p_{T,\mathrm{total}}^2$. Here, M_Z is the Z boson mass and $p_{T,\mathrm{total}}$ is the scalar sum of the transverse momentum for all the jets with $p_T^{\mathrm{jet}} > 20$ GeV and $|\eta| < 2.5$ in the event. Corrections are applied to account for non-perturbative effects, on the order of 5%, estimated using the ALPGEN+PYTHIA simulation. The NLO pQCD predictions of $R_{c/\mathrm{jet}} = 0.0368$ and $R_{c/b} = 1.64$ [1] disagree significantly with the measurements. In the case where the intrinsic charm of the proton is enhanced, as suggested in the CTEQ6.6c PDF sets [13], MCFM yields ratios of $R_{c/\mathrm{jet}} = 0.0425$ and $R_{c/b} = 2.23$, which are still in disagreement with our data.

The uncertainty on the $R_{c/\mathrm{jet}}$ theoretical predictions are evaluated by simultaneously changing the μ_R and μ_F scales up and down by a factor of two, yielding an uncertainty of up to 11% on $R_{c/\mathrm{jet}}$, while this uncertainty cancels in $R_{c/b}$. However, this uncertainty is smaller than the effect due to the intrinsic charm enhancement, which is 15% and 36% for $R_{c/\mathrm{jet}}$ and $R_{c/b}$, respectively.

ALPGEN generates multi-parton final states using tree-level MEs. When interfaced with PYTHIA, it employs the MLM scheme [22] to match ME partons with those after showering in PYTHIA, resulting in an improvement over leading-logarithmic accuracy.

SHERPA uses the CKKW matching scheme between the leading-order ME partons and the parton-shower jets following the prescription given in Ref. [23]. This effectively allows for a consistent combination of the ME and parton shower.

PYTHIA includes only $2 \to 2$ MEs with $gQ \to ZQ$ and $q\bar{q} \to Zg$ scatterings followed by $g \to Q\bar{Q}$ splitting, where Q is either a b or c quark. The Perugia0 tune [24] and the CTEQ6L1 PDF set are used for the PYTHIA predictions.

The ratios of differential cross sections as a function of $p_T^{\rm jet}$ and p_T^Z are compared to various predictions in Fig. 2. On average, the NLO predictions significantly underestimate the data, by a factor of 2.5 for the integrated results. As for the MC event generators, PYTHIA predictions are closer to data. An improved description can be achieved by enhancing the default rate of $g \to c\bar{c}$ in PYTHIA by a factor of 1.7, motivated by the $\gamma + c$ jet production measurements at the Tevatron [25, 26].

The largest discrepancy between data and predictions, in particular for the shape of the differential distributions, is for $R_{c/b}$ as a function of p_T^Z (Fig. 2(d)). The level of disagreement in shape is quantified for the MCFM NLO prediction when its integrated result is scaled up to match the data. We generated a large number of pseudo-experiments and found the p-value for the four bins in p_T^Z to simultaneously fluctuate to the observed $R_{c/b}$ values (or beyond) to be 2%.

We have presented the first measurements of the ratios of integrated cross sections, $\sigma(p\bar{p} \to Z + c \text{ jet})/\sigma(p\bar{p} \to Z + \text{jet})$ and $\sigma(p\bar{p} \to Z + c \text{ jet})/\sigma(p\bar{p} \to Z + b \text{ jet})$, as well as the ratios of the differential cross sections in bins of $p_T^{\rm jet}$ and p_T^Z, for events with a Z boson decaying to electrons or muons and at least one jet in the final state. Measurements are based on the data sample collected by the D0 experiment in Run II of the Tevatron, corresponding to an integrated luminosity of 9.7 fb^{-1} at a center-of-mass energy of 1.96 TeV. For jets with $p_T^{\rm jet} > 20$ GeV and $|\eta^{\rm jet}| < 2.5$, the measured integrated ratios are $R_{c/\rm jet} = 0.0829 \pm 0.0052\,(\text{stat.}) \pm 0.0089\,(\text{syst.})$, and $R_{c/b} = 4.00 \pm 0.21\,(\text{stat.}) \pm 0.58\,(\text{syst.})$. The NLO pQCD predictions disagree significantly with the results. PYTHIA agrees better with the measured ratios, especially when the gluon splitting to $c\bar{c}$ pairs is enhanced.

We thank the authors of Refs. [1, 20] for valuable discussions, and the staffs at Fermilab, and collaborating institutions, and acknowledge support from the DOE and NSF (USA); CEA and CNRS/IN2P3 (France); MON, NRC KI and RFBR (Russia); CNPq, FAPERJ, FAPESP and FUNDUNESP (Brazil); DAE and DST (India); Colciencias (Colombia); CONACyT (Mexico); NRF (Korea); FOM (The Netherlands); STFC and the Royal Society (United Kingdom); MSMT and GACR (Czech Republic); BMBF and DFG (Germany); SFI (Ireland); The Swedish Research Council (Sweden); and CAS and CNSF (China).

[1] J. M. Campbell, R. K. Ellis, F. Maltoni, and S. Willenbrock, Phys. Rev. D **69**, 074021 (2004).
[2] V. M. Abazov *et al.* (D0 Collaboration), Phys. Rev. Lett. **109**, 121803 (2012); T. Aaltonen *et al.* (CDF Collaboration), Phys. Rev. Lett. **109**, 111803 (2012).
[3] A. Abulencia *et al.* (CDF Collaboration), Phys. Rev. D **74**, 032008 (2006).
[4] T. Aaltonen *et al.* (CDF Collaboration), Phys. Rev. D **79**, 052008 (2009).
[5] V. M. Abazov *et al.* (D0 Collaboration), Phys. Rev. Lett. **94**, 161801 (2005).
[6] V. M. Abazov *et al.* (D0 Collaboration), Phys. Rev. D **87**, 092010 (2013).
[7] V.M. Abazov *et al.* (D0 Collaboration), Nucl. Instrum. Methods Phys. Res. A **565**, 463 (2006); M. Abolins *et al.*, Nucl. Instrum. Methods Phys. Res. A **584**, 75 (2008); R. Angstadt *et al.*, Nucl. Instrum. Methods Phys. Res. A **622**, 298 (2010).
[8] Pseudorapidity is defined as $\eta = -\ln[\tan(\theta/2)]$, with the polar angle θ measured relative to the proton beam direction.
[9] G. C. Blazey *et al.*, arXiv:hep-ex/0005012.
[10] M. L. Mangano *et al.*, J. High Energy Phys. **07** (2003) 001. Version 2.11 was used.
[11] T. Sjöstrand, S. Mrenna, and P. Skands, J. High Energy Phys. **05** (2006) 026. Version 6.409 was used.
[12] D. J. Lange, Nucl. Instrum. Meth. Phys. Res. A **462**, 152 (2001).
[13] J. Pumplin *et al.*, J. High Energy Phys. **07** (2002) 012.
[14] J. M. Campbell and R. K. Ellis, Phys. Rev. D **60**, 113006 (1999); ibid. **62**, 114012 (2000); ibid. **65**, 113007 (2002).
[15] U. Langenfeld, S. Moch, and P. Uwer, Phys. Rev. D **80**, 054009 (2009).
[16] V. M. Abazov *et al.* (D0 Collaboration), Phys. Rev. Lett. **100**, 102002 (2008).
[17] V. M. Abazov *et al.* (D0 Collaboration), Nucl. Instrum. Methods Phys. Res. Sect. A **620**, 490 (2010). V. M. Abazov *et al.* (D0 Collaboration), to be submitted to Nucl. Instrum. Methods Phys. Res. A.
[18] A. Hoecker, P. Speckmayer, J. Stelzer, J. Therhaag, E. von Toerne, and H. Voss, "TMVA: Toolkit for Multivariate Data Analysis," PoS A CAT 040 (2007) [physics/0703039].
[19] G.D. Lafferty, and T.R. Wyatt, Nucl. Instrum. Methods Phys. Res. Sect. A **355**, 541 (1995).
[20] T. Gleisberg *et al.*, J. High Energy Phys. **02** (2009) 007.
[21] A. D. Martin, W. J. Stirling, R. S. Thorne, and G. Watt, Eur. Phys. J. C **63**, 189 (2009).
[22] F. Caravaglios *et al.*, Nucl. Phys. **B539**, 215 (1999).
[23] S. Catani *et al.*, J. High Energy Phys. **11** (2001) 063. Version 1.3.1 was used.
[24] P. Z. Skands, Phys. Rev. D **82**, 074018 (2010).
[25] V. M. Abazov *et al.* (D0 Collaboration), Phys. Lett. B **719**, 354 (2013).
[26] T. Aaltonen *et al.* (CDF Collaboration), Phys. Rev. Lett. **111**, 042003 (2013).